A New Intermolecular Polarizable Potential for a Formaldehyde Dimer. Application to Liquid Simulations

Jose M. Hermida-Ramón* and Miguel A. Ríos

Departamento de Química Física, Facultad de Química, Universidad de Santiago de Compostela, Avda das Ciencias S/N, E-15076 Santiago de Compostela, Spain

Received: July 13, 1998; In Final Form: September 30, 1998

An intermolecular potential for a formaldehyde dimer that includes many body effects was constructed from the monomer properties and intermolecular perturbation theory calculations. The interaction energy was calculated as a sum of various terms with physical significance. A global minimum of C_s symmetry similar to that arrived at from experimental calculations was predicted for the dimer; its calculated energy, −3.82 kcal/mol, is comparable to that provided by ab initio MP2/6-31G++(2d,2p) calculations (−3.54 kcal/mol). Stationary points for the trimer were preliminarily explored; the geometries obtained contained a variable number of hydrogen bonds and exhibited differences in the nature of their interactions. A molecular dynamics method was used to simulate the liquid phase of formaldehyde; a first-coordination sphere containing about 13 molecules that remained quite structured even at fairly long distances was obtained.

Introduction

In recent years, a large number of ab initio potentials for a wide variety of molecules[1−8] including the formaldehyde−water dimer[9−15] have been reported; by contrast, no similar values appear to have been published for the formaldehyde dimer. To a lesser extent, the formaldehyde dimer has been studied by using various methods including microwave,[16] IR,[17] and Raman spectroscopies[18] and subjected to different theoretical computations.[19−23] Most of these studies have led to a conformation of C_s symmetry such as that of Figure 1a for the dimer. No calculations or theoretical potential values for aggregate conformations larger than the dimer have seemingly been reported, nor have any studies in the liquid phase—only in the solid state.[24] A study of the interaction between two formaldehyde molecules and its extension to the liquid phase provides insight into the behavior of the formaldehyde liquid phase. Another, even more important, reason for developing a potential for formaldehyde is that it can be uses in formaldehyde−water simulations, thus contributing to the assessment of the role of formaldehyde−formaldehyde iterations in the formaldehyde−water system.

We chose the perturbational method[25−27] among the most widely used for studying molecular interactions; we preferred it to the supermolecule method[28] to obtain the proposed formaldehyde potential. Both alternatives have their merits and pitfalls, however. For instance, the supermolecule method is fairly easy to apply but has several shortcomings such as the difficulty to include many-body effects[29,30] in a straightforward way and the problems posed by the basis set superposition error (BSSE),[31,32] which entails using a counterpoise correction[33] that further increases the already large number of computations involved in this method. The time needed to explore the potential surface increases considerably if the method is to include electron correlation. One other disadvantage of this method is that is sheds little light on the nature of contributions to the intermolecular energy values it provides as the fitted parameters of the potential function obtained cannot be directly assigned to specific physical properties. This originates that properties that were not considered in the fitting of the function may be unreliably predicted. With a potential such as that proposed in this study, this previous problem is substantially reduced.

In this work, we constructed a potential for the formaldehyde dimer, some terms of which were derived from the monomer properties. It is important that high-level quantum and perturbation treatments of molecular interactions are investigated for a chemically interesting system in order to establish benchmarks for force field developments. Also, in this study we simplify the potential to be used in liquid-phase simulation, including essentially a more or less exact and extensive description of the electrostatic term, but it also permits us to evaluate the extent to which this description may be simplified without an important loss of realiability of the potential. To develop the potential, we used perturbational computations of the dimer provided by the Hayes−Stone intermolecular perturbation theory (IMPT).[27,34,35] This treatment accounts for short-range effects such as the overlap of wave functions and nonorthogonality in the dimer wave functions. The perturbational theory expresses the interaction energy as a series of terms of variable order;[25] we used first- and second-order terms only. In the previous context, the intermolecular energy for the potential is expressed as a combination of several terms of first and second order that represent contributions with physical significance:

$$E_{\mathrm{int}} = E_{\mathrm{elec}} + E_{\mathrm{ind}} + E_{\mathrm{rep}} + E_{\mathrm{disp}} \qquad (1)$$

where E_{elec} is the electrostatic energy, E_{ind} the induction energy, E_{rep} the repulsion energy—which includes exchange terms and potential errors of prediction in the previous terms arising from the exclusion of overlapping—, and E_{disp} is the dispersion energy.

Many-body effects are considered in the induction energy,[29,30] which, for an individual molecule, depends on the relative position of the others in the system concerned. This effect is specially significant in condensed-phase simulations.

To establish a compromise between the computational cost derived from the calculation level used and the accuracy of the results obtained, we chose to use the 6-31G++(2d,2p) basis

10.1021/jp982987l CCC: $15.00
Published on Web 12/03/1998

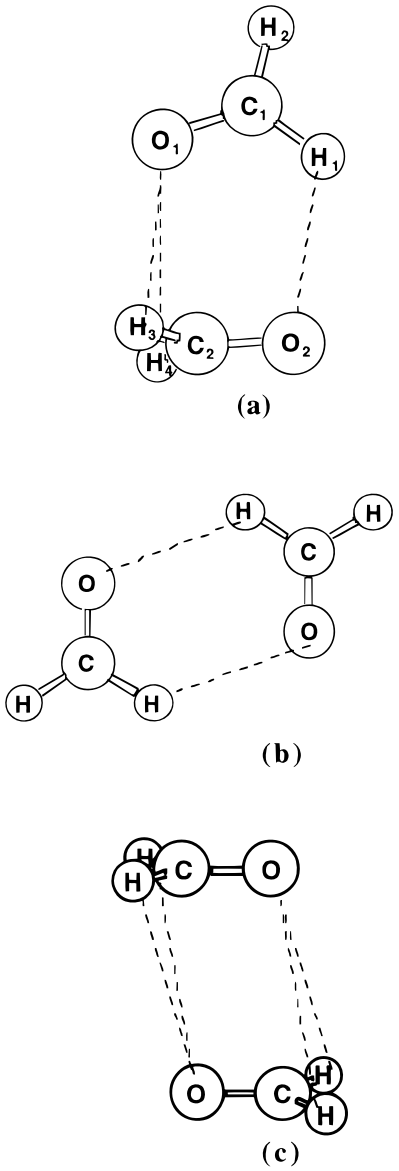

Figure 1. Conformations used to test the potencial. (a) C_s conformation. (b) C_{2h} Planar conformation. (c) C_{2h} antiparallel conformation.

set. Del Bene[36] has shown that a similar basis set [6-31+G-(2d,2p)] at the MP2 level is appropriate for studying H-bonding complexes; we also found in a previous study[37] for acetone that it was necessary to include electronic correlation and diffuse functions to predict reliable dimer energies. Also, the experimental geometry of the monomer was adopted.[16] Table 1 shows the values of some electrical properties provided by this basis set, together with their experimental[38] counterparts and the results provided by a Sadlej[39] basis set, viz. (10s6p4d/6s4p)/[5s3p2d/3s2p], which usually represents these properties quite accurately. As can be seen, the dipole moment obtained at the HF level was too high; with electron correlation, however, the value was only 2% larger than its experimental counterpart. However, polarizability values were slightly better in the absence of electron correlation, in contradiction to the usual trend.

Ab initio calculations were performed by using two software packages: CADPAC[40] for IMPT computations, distributed dipole moment analysis (DMA),[41,42] and distributed polarizability calculations;[43] GAUSSIAN94[44] for additional computations.

The potential thus developed was tested by using it to compute different stationary points for the formaldehyde dimer.

TABLE 1: Experimental and Ab Initio Molecular Dipoles (D), Quadrupoles (au), and Polarizabilities (au)[a]

	experimental[b]	631++G(2d,2p)	Sadlej
μ_z	2.33	2.38 (SCF 2.89)	2.32
Q_{xx}	$+0.2 \pm 0.2$	0.042 (SCF 0.158)	0.061
Q_{yy}	-0.1 ± 0.5	0.097 (SCF -0.166)	0.167
Q_{zz}	-0.1 ± 0.3	-0.139 (SCF 0.008)	-0.228
P_{xx}		15.79 (SCF 15.25)	17.21
P_{yy}		10.45 (SCF 10.39)	12.62
P_{zz}		19.23 (SCF 20.72)	20.04
$P_{aver.}$	16.53; 16.94	15.18 (SCF 15.45)	16.60

[a] Ab Initio calculations at the MP2/631++G(2d,2p) level and at the MP2 level using a Sadlej basis set. The atomic Cartesian coordinates (bohr) used in the calculations are: C (0.0, 0.0, 0.0), O (0.0, 0.0, 2.2771), H_1 (1.7800, 0.0, -1.1097), and H_2 (-1.7800, 0.0, -1.1097). [b] Reference 38.

At a later stage, calculations were also applied to the trimer. Finally, the liquid phase of formaldehyde was simulated by using a molecular dynamics method[45] and a simplified version of the original potential.

Description of the Potential

As noted earlier, the intermolecular energy surface was explored by using the IMPT method, which considers the overlap of charge clouds and antisymmetry in the dimer wave function. Energies IMPT ab initio of the order up to 2 were obtained for overall 259 randomly chosen configurations with carbon distances in the range 5−12.75 bohr. The monomer geometry was kept constant and experimental values were adopted in all calculations. The models used to represent each component of the interaction energy are described below.

Electrostatic Energy. This type of energy, which results from interactions among molecular charge distributions, is possibly the most important in polar molecules containing elements in the second row of the periodic table, so it must be modeled rigorously. At long distances, the electrostatic energy parametrized by a multipole expansion is similar to that provided by the IMPT theory because the overlapping effects of monomer wave functions considered by this theory are negligible at such distances. The overlapping effects at short distances were considered in parametrizing the repulsion energy. We used a multipole expansion over the different atoms in order to improve the expansion convergence. These multipoles are calculated with the Stone's DMA[41,42] method. So the electrostatic term[46] for two molecules A and B is

$$E_{\text{elec}} = Q_t^{\text{A}} T_{tu}^{\text{AB}} Q_u^{\text{B}} \qquad (2)$$

where u and t are momentum angular labels 00,10,10c,11s, 20..., Q are the diferent multipoles, and T are tensors to introduce the orientation between the molecules. T depend only on the relative positions of the molecular axis system, so they can be evaluated once and for all; they are given elsewhere.[47]

Table 2 shows the multipoles with order up to 4 as obtained at the MP2 level. We adopted this expansion rather than the SCF one because, as shown in Table 1, SCF multipoles were too high. In this way, an electrostatic energy at the correlated level was obtained, which, however, did not include overlapping effects.

To obtain the simplified version of the potential needed to simulate the condensed phase, the expansion was truncated at the dipole. The resulting error was determined from electrostatic

TABLE 2: Nonzero Real Components of the Atomic Multipole Moments (Spherical Tensors in Atomic Units) at the MP2 Level[a]

Carbon (at $x = 0.0$, $y = 0.0$, $z = 0.0$)				
Q_{00} 0.551177				
Q_{10} 0.328671				
Q_{20} 0.121991	Q_{22c} −0.374377			
Q_{30} −0.815973	Q_{32c} 2.204095			
Q_{40} 1.837796	Q_{42c} −0.554732	Q_{44c} −0.005666		
Oxygen (at $x = 0.0$, $y = 0.0$, $z = 2.2771$)				
Q_{00} −0.482998				
Q_{10} −0.028507				
Q_{20} 0.322600	Q_{22c} −0.443326			
Q_{30} −0.165051	Q_{32c} −0.717132			
Q_{40} 0.490107	Q_{42c} 1.037968	Q_{44c} −0.040217		
Hydrogen (at $x = 1.7800$, $y = 0.0$, z = −1.1097)				
Q_{00} −0.034090				
Q_{10} −0.107040	Q_{11c} 0.174875			
Q_{20} 0.018582	Q_{21c} 0.085319	Q_{22c} −0.052754		
Q_{30} 0.039052	Q_{31c} 0.012535	Q_{32c} −0.037298	Q_{33c} 0.009118	
Q_{40} 0.021911	Q_{41c} −0.011776	Q_{42c} −0.010481	Q_{43c} −0.001747	Q_{44c} 0.013023

[a] The multipoles for H_2 are given by $Q_{lmc}(H_2) = (-1)^m Q_{lmc}(H_1)$.

TABLE 3: Nonzero Atomic Dipole Polarizabilities (Cartesian Tensors in Atomic Units) at the MP2 Level by Using the Same Coordinate System as Above[a]

	P_{xx}	P_{yy}	P_{zz}	P_{xz}	P_{zx}	$P_{average}$
C	6.23	4.88	7.98	0.00	0.00	6.36
O	3.87	4.02	7.44	0.00	0.00	5.11
H_1	2.85	0.77	1.90	−1.30	−1.12	1.84

[a] Diagonal terms for H_2 are equal to H_1 terms, nondiagonal terms have opposite signs.

energy calculations obtained by using the classical expression (eq 2) and by applying both multipole expansions (up hexadecapole and up dipole) to an overall 405 points with distances between the central carbon atoms longer than 3.5 Å. After exclusion of exceedingly repulsive points, an root mean square (RMS) of 0.65 mH between both expansions was obtained. On the basis of the typical errors of the method, this approach was considered suitable for the condensed phase.

Induction Energy. Induction energy stems from the distortion of the charge of a molecule by the electrical field of neighboring molecules. In calculating our potential, this energy was parametrized through the distributed anisotropic polarizabilities[43] (DP) over the atoms. These polarizabilities interact with the multipole expansion for the other molecules by way of the field produced by the expansions. So the induction energy is[46]

$$E_{\text{ind}} = \frac{1}{2} \sum_{\text{A}} \sum_{\text{B}\neq\text{A}} \Delta Q_t^a T_{tu}^{ab} Q_u^b \tag{3}$$

The induced moments are expressed by

$$\Delta Q_t^a = -\sum_{\text{B}\neq\text{A}} \alpha_{tt'}^{aa'} T_{t'u}^{a'b} (Q_u^b + \Delta Q_u^b) \tag{4}$$

α are the polarizabilities obtained by DP. The induced moments that appear in this expression depend on the induced moments of the neighbor molecules. This problem commonly is resolved by an iterative procedure. By adopting explicit polarizabilities, we included most of the many-body effects in the system.

Table 3 gives the distributed polarizabilities for the atoms as calculated by CADPAC. As can be seen from Table 1, the polarizability yielded by our calculations was slightly smaller than the experimental value; the difference, however, allows one to use the atomic polarizabilities of Table 3 in the potential.

The IMPT method also provides the charge-transfer energy for each configuration. This energy is closely related to the polarization energy. However, whether it should be included in intermolecular potentials remains a subject of debate.[29] It was about 0.7 mH in the most attractive configurations—those with the greatest charge transfers among the configurations of interest—, so we chose not to include it in the potential.

Repulsion Energy. As noted earlier, in addition to the repulsion term resulting from the Pauli exclusion principle, this energy includes others such as that corresponding to the possible exchange of electrons belonging to different molecules and the penetration energy due to the overlap of the monomer charge clouds. The exchange−repulsion energy is repulsive and decays in an exponential manner. The penetration energy is also an exponential function. On the basis of this behavior, the energies were modeled by the following expression:[48]

$$E_{\text{rep}} = \sum_{ij} \text{e}^{-\alpha_{ij}(r_{ij} - \rho_{ij})} \tag{5}$$

where subscripts i and j denote atoms and α_{ij} and ρ_{ij} are two adjustable parameters that depend on the particular pair of interacting atoms. α and ρ were fitted from 259 IMPT calculations for the formaldehyde dimer. Elimination of the points with energies above 30 mH led to an overall 222 configurations in the fit. The energy values used were obtained from

$$E_{\text{rep}} = E_{\text{exch-rep}}(\text{IMPT}) + E_{\text{elec}}(\text{IMPT}) - E_{\text{elec}}(\text{DMA}) \tag{6}$$

where $E_{\text{exch-rep}}$ is the exchange−repulsion energy provided by the IMPT method, E_{elec} (IMPT) is the ab initio electrostatic energy, and E_{elec} (DMA) is the electrostatic energy obtained by using distributed multipoles at the SCF level. Equation 3 considers the difference between the ab initio electrostatic energy and that modeled by multipole expansion (i.e., the overlap term of the electrostatic energy).

Data were fitted to a weighted function in order to favor the more attractive configurations, with a weight $w(E) = \exp(-E/p)$, $p = 0.8$ mH and E as the interaction energy for each configuration, which was taken to be the sum of E_{elec}-(DMA, MP2), E_{rep}(eq 3), E_{ind}(DMA, DP, MP2), and E_{disp}-(IMPT). The RMS thus obtained was 0.136 mH.

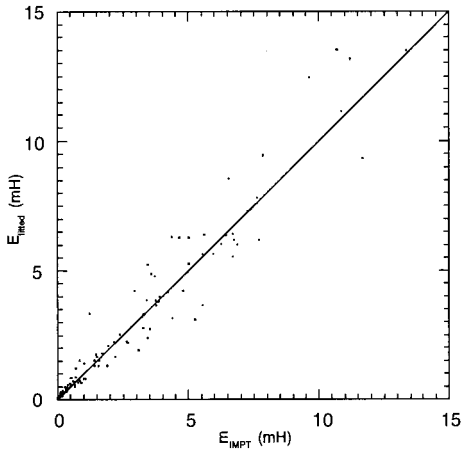

Figure 2. Fit of repulsion energy to eq 3.

TABLE 4: Parameters and RMS for the Different Exchange−Repulsion Energy Fits (α in bohr^{-1}, ρ in bohr, and RMS in mH)

	hexadecapole potential		dipole potential	
RMS	0.136249		0.178449	
	α	ρ	α	ρ
C−C	1.82925	6.46586	2.00515	6.31618
C−O	1.07668	5.13041	7.97466	1.13449
C−H	5.09304	1.06867	1.44432	5.00812
O−O	2.39389	6.11264	2.04498	5.55819
O−H	2.28140	4.76031	2.37978	4.97952
H−H	1.92456	4.45179	2.69714	3.63777

In several studies,[4,29,48] parameter ρ has been expressed as a function of orientation-depending quantities in order to consider atomic anisotropy. We performed fittings with first-order spherical harmonics. Fits were not much better and the number of parameters increased as a result. Therefore, although using higher order spherical harmonics increased the goodness of fit, the RMS provided by an isotropic model was judged good enough, so raising computational costs by using a larger number of parameters to calculate the energy was deemed not necessary.

Table 4 gives the parameter values and RMS obtained from the fits with each of the electrostatic models (up to the hexadecapole and up to the dipole). Figure 2 compares the energies predicted by eq 3 from the IMPT calculations with those obtained by fitting. As can be seen, the latter provided satisfactory repulsion energies, which, however, were less accurate in the presence of strong repulsions.

Dispersion Energy. The dispersion energy was parametrized from the following London expression:[6,30,38]

$$E_{\text{disp}} = \frac{3}{2} C \frac{E_1 E_2}{E_1 + E_2} \sum_{m,n}^{\text{atoms}} f_{mn} \alpha_m \alpha_n r_{mn}^{-6} \tag{7}$$

where E_1 and E_2 are the molecular ionization potentials, which, on the basis of Koopman's theorem, correspond to the energy of the highest occupied molecular orbital in each molecule; α denotes the spherical polarizabilities of the atoms; f_{mn} is a damping function intended to include overlapping effects on dispersion and given by the equation of Tang and Toennis:[49]

$$f_{mn} = 1 - e^{-ar_{mn}} \sum_{k=0}^{6} \frac{(ar_{mn})^k}{k!} \tag{8}$$

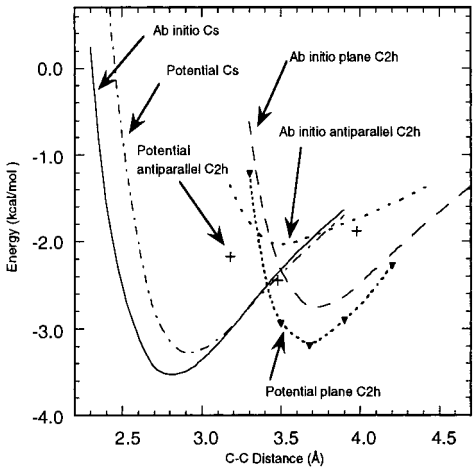

Figure 3. Comparison of the intermolecular interaction energy predicted by the proposed model and the results of calculations at the MP2/631++G(2d,2p) level.

TABLE 5: Atomic Dispersion Coefficients in Atomic Units

atoms pairs	C_{ij}	atoms pairs	C_{ij}
C−C	35.5638	O−O	22.9581
C−O	28.5741	O−H	8.2667
C−H	10.2889	H−H	2.9767

r_{mn} being the distance between both atoms and parameter a being related to the hardness of the atoms that form the molecule—its value was estimated from the mean of α values for the repulsion energy fitting,[4] approximated to 2.5 in order to increase the damping effect at short distances. A correction factor C that was parametrized from a fit of 222 different conformations was included in eq 4 together with an appropriate a value in order to decrease the RMS and improve predicted dispersion energies near minima. The final value of C was 2.65 and that of the RMS 0.341 mH. Table 5 gives the C_{mn} coefficients for the different atoms, calculated from

$$C_{mn} = \frac{3}{2} C \frac{E_1 E_2}{E_1 + E_2} \alpha_m \alpha_n \tag{9}$$

To determine to what extent the goodness of fit suffered in adopting the above-described model, the energies for the 222 conformations were fitted to equations of the types

$$E_{\text{disp}} = \sum_{m,n}^{\text{atoms}} B_{mn} r_{mn}^{-6} \tag{10}$$

and

$$E_{\text{disp}} = \sum_{m,n}^{\text{atoms}} D_{mn} r_{\text{mn}}^{-6} f_{mn} \tag{11}$$

where B_{mn} and D_{mn} are two fitted parameters for each atom pair. Neither equation provided a significantly improved RMS; also, parameter values fluctuated over wide ranges, so we chose to preserve a clearer physical significance rather than improve the fit to an insignificant extent.

Figure 3 compares the interaction energy of the potential with that obtained from supermolecule calculations at the MP2 level for the three configurations depicted in Figure 1. It should be noted that the comparison is only semiquantitative since, although the correlation in the charge fluctuations via the IMPT dispersion energy was included, this energy did not consider

TABLE 6: Distances (Å), Angles (deg), and Energies (kcal/mol) for C_s Minimum (One Monomer Is Normal to the Symmetry Plane)

	exp. 1[a]	exp. 2[a]	exp. 3[b]	631++G(2d,2p)[c]	631++G(2d,2p)[d]	aug-cc-pTVZ[e]	potential **1**[f]	potential **2**[f]
r_{C-C}	3.005	3.500		3.1717	3.1546		3.3370	3.2893
$r_{O_2-H_1}$	2.18(13)	2.46(10)	2.4668	2.4312	2.4059		3.2153	2.8162
r_{C_2-O1}	2.98(8)	2.82(10)	2.7531	2.7206	2.7016		2.5740	2.4791
$\alpha_{O_1C_1C_2}$	75.6	58.3		57.5	57.4		42.2	39.4
$\alpha_{O_2C_2C_1}$	111.2	90.1		77.1	77.1	93.5	74.1	
$E_{Tot.}$				−3.54	−3.68	−4.08	-3.82	-4.24

[a] Microwave data, ref 16. [b] Crystal structure, ref 24. [c] Intermolecular coordinates optimization. [d] Full optimization. [e] Single-point calculation at the intermolecular minimum. [f] Potential **1** multipole expansion up to hexadecapole. Potential **2** multipole expansion up to dipole.

TABLE 7: Distances (Å), Angles (deg), and Energies (kcal/mol) for Minimum with a C_{2h} Planar Geometry

	631++G(2d,2p)[a]	631++G(2d,2p)[b]	aug-cc-pTVZ[c]	potential **1**[d]	potential **2**[d]
r_{C-C}	3.6797	3.6488		3.5948	3.7693
r_{O-H}	2.5626	2.5304		2.5034	2.6438
α_{OCC}	62.9	64.7		68.6	58.8
$E_{Tot.}$	−2.78	−3.06	−3.15	−3.41	−3.43

[a] Intermolecular coordinates optimization. [b] Full optimization. [c] Single-point calculation at the intermolecular minimum. [d] Potential **1** multipole expansion up to hexadecapole. Potential **2** multipole expansion up to dipole.

intramolecular correlation energy, which was to a large extent included in the MP2 computations. Although the curves are similarly shaped, there are deviations at the shorter distances; thus, the potential produces a less deep well than that resulting from the MP2 calculations for the orthogonal configuration and the opposite holds true for the parallel configurations. These differences can be ascribed both to the above-mentioned fact that intramolecular correlation was not considered and to errors in modeling overlapping effects. These effects will increase with decreasing distance. One other reason might be that the repulsion energy for the orthogonal configuration is overestimated whereas those for the parallel conformations are underestimated. We should note that, as shown later on, the global minimum obtained for the parallel conformations is very close to the configurations of Figure 3; however, angle variations in the orthogonal configuration displace it slightly from the line predicted by the supermolecule calculations. In any case, the energy difference between the two potential minima is similar to that between the MP2 minima.

The Simplified Potential

Tables 2−5 show all the parameters for the different terms that provided the simplified potential used in simulating the liquid phase or formaldehyde. As stated above, a multipole expansion as far as the dipole and distributed polarizabilities were used to represent the electrostatic and induction energies. The repulsion parameters given in Table 4 were fitted similarly to the hexadecapole. However, p in the weighting function was taken to be 2.5 and E was identified with the repulsion energy. These changes were intended to produce a function that would accurately fit conformations with intermediate repulsion energies at the expense of strongly attractive conformations. The damping function in the dispersion term was simplified for the simulation. The Tang and Toennis function[49] was adjusted to

$$f_{mn} = 1 - e^{-(c \cdot r)^n} \qquad (12)$$

with $c = 0.3247$, $n = 3$, and RMS $= 1.99 \times 10^{-4}$. We shall henceforward refer to the potential obtained from the multipole expansion up to the hexadecapole as potential **1** and to the simplified potential (encompassing up to the dipole only) as potential **2**.

Gas-Phase Calculations

The accuracy of the calculated potentials was checked by exploring the dimer surface in order to obtain formaldehyde minima, using the program ORIENT.[50] The results were compared with reported experimental values and ab initio calculations at the MP2/6-31G++(2d,2p) level including counterpoise correction.

Experimental studies[16−18] have predicted a structure of C_s symmetry such as that of Figure 1 for the formaldehyde dimer. Relatively old and theoretical calculations at low computational levels predicted a planar structure of C_{2h} symmetry (Figure 1) as the lowest-energy conformation—the C_s structure was predicted to have a higher energy. On the other hand, in a recent study using the 6-31++G** basis set at the MP2 level, Ford et al.[23] predicted three minima for this dimer—some of the energies, in kJ/mol, reported by these authors were apparently inconsistent with their own atomic units values, namely, a minimum of more negative energy of C_s symmetry, a less stable one of C_{2h} symmetry, and a C_{2v} minimum with the least negative energy of all three. This third minimum possessed a head-to-tail conformation in which the four atoms involved in the double bonds lay in a straight line and the two molecular planes are at an angle of 90°.

The exploration conducted with both potentials gave a more stable minimum of C_s symmetry in both cases, followed by another of C_{2h} symmetry and with a cyclic geometry. This kind of cyclic structure appears as the global minimum in other complexes containing a carbonyl group.[51] Instead of the C_{2v} minimum obtained by Ford et al., we detected a stationary point of variable order depending on the potential used. To check the reliability of the potentials in relation to this head-to-tail conformation, we performed an ab initio optimization at the MP2/6-31++G(2d,2p) level, using relaxed coordinates. This calculation predicted the head-to-tail conformation as a transition state.

Tables 6 and 7 show the experimental results and those obtained from the ab initio calculations or provided by the two potentials for the C_s and C_{2h} minima, respectively. Ab initio calculations were carried out by maintaining the experimental geometry of the monomer and optimizing intermolecular parameters only; optimizations that included all (intra- and intermolecular) coordinates were also performed. As can be seen from the different geometries for the C_s conformation, the C−C

TABLE 8: Intermolecular Energy Components for the C_s and C_{2h} Minima (kcal/mol)

	C_s minimum		C_{2h} minimum	
	potential **1**[a]	potential **2**[a]	potential **1**[a]	potential **2**[a]
$E_{elec.}$	−3.38	−2.91	−2.94	−2.82
$E_{ind.}$	−0.55	−0.51	−0.46	−0.34
$E_{rep.}$	3.39	3.29	2.30	1.68
$E_{disp.}$	−3.26	−4.12	−2.31	−1.94
$E_{Tot.}$	−3.82	−4.24	−3.41	−3.43

[a] Potential **1** multipole expansion up to hexadecapole. Potential **2** multipole expansion up to dipole.

distances obtained from the ab initio calculations and those predicted from the potentials that can be used as the center of the molecular framework fall within the ranges of the microwave results.[16] Consistency, however, is poorer at other distances. A similar conclusion can be drawn from the angles. In particular, in Table 6 the distance O_2-H_1 is too long; this is due, on one hand, to a rotation of molecule 1 over an axis containing the C_1 atom and perpendicular to the molecular plane, and, on the other hand, to an increase of the value of the angle that defines the position of the C_1 atom with respect to the C−O bond of the second molecule. This change gives a lengthening of the O_2-H_1 distance and a shortening of the C_2-O_1 and also H_3-O_1 and H_4-O_1 distances. The main reason for the disagreement between the potential and the ab initio data may be one deficiency in the description of the anisotropy in the repulsion, which increases the C−C and reduces the O−C repulsion for these orientations. The energies of the minima derived from the potentials are generally more negative than those provided by the ab initio calculations. These may be due to the need to include greater anisotropy or damping in some terms, as well as intramolecular correlation. We performed specific calculations for the geometries of the intermolecular minima, using a larger basis set; from the results it seemingly follows that the potentials overestimate the energy for the C_{2h} conformation to a greater extent than that for the C_s conformation. We should note that the energy change produced by relaxing all coordinates was more marked in the planar conformation than in the C_s conformation.

Table 8 gives the values for the different energy components of both minima. As shown by this table, the electrostatic and dispersion energies for the C_s conformation were roughly equally significant, consistent with previous findings[16,23,52] that, in addition to its electrostatic character, this conformation exhibits an effect arising from van der Waals forces between O_1 and C_2. As can also be seen from the table, the combined energies—the dispersion term excluded—lead to the C_{2h} conformation as the lowest-energy minimum, consistent with previous SCF calculations and the IMPT results, where the sum of the first-order energies for the C_{2h} conformation was more negative than that for C_s.

A preliminary exploration in search of minima of the formaldehyde trimer was done by using the modeled potentials. The points thus obtained were compared with those provided by the ab initio calculations, with and without a fixed monomer geometry. Rather than an exhaustive search for stationary points of the trimer, these computations were intended to check our potentials with complexes with an order greater than 2. Tables 9 and 10 give the BSSE corrected energies and the geometries for the stationary points shown in Figure 4. The figure shows two types of positions of the oxygen atom relative to the neighboring molecule. In one, the oxygen atom lies at the same distance from both hydrogens in the neighbor, in the plane that bisects the angle formed between the two hydrogens and the carbon. In the other position, the oxygen atom is closer to one hydrogen, in the same plane as the neighboring molecule. We shall refer to this latter arrangement as *planar bond*. This kind of interaction, C−H···O, being defined as hydrogen bond.[53,54]

The geometries predicted by potential **1** are more accurate than those predicted by potential **2**. Apparently, this is not the case with the conformations containing one or two *planar bonds* (Figures **4c** and **4d**). In these conformations, however, the distances that determine the character of the intermolecular interaction (viz. O···H for a *planar bond* and C···O in its absence) are more accurately represented by model **1**. Both potentials predict the same energy sequence as the ab initio calculations performed with a fixed monomer geometry. However, the sequence changes when all the coordinates are relaxed

TABLE 9: Distances (Å), Angles (deg), and Corrected Energies (kcal/mol) for a Formaldehyde Trimer (Conformations with 3 and 0 *Planar Bonds*[a])

	NO *planar bonds*[a]				three *planar bonds*[a]			
	potential **2**[b]	potential **1**[b]	631++G(2d,2p)[c]	631++G(2d,2p)[d]	potential **2**[b]	potential **1**[b]	631++G(2d,2p)[c]	631++G(2d,2p)[d]
$r_{C_1-C_5}$	3.4146	3.4464	3.7033	3.7059	4.5397	4.2247	4.3267	4.2400
$r_{C_5-C_9}$	3.4146	3.4464	3.7131	3.7024	4.5397	4.2247	4.2645	4.3012
$\alpha_{O_2-C_1-C_5}$	84.1	97.1	95.0	95.3	93.6	105.3	103.0	102.6
$\alpha_{O_6-C_5-C_9}$	84.1	97.1	96.0	95.7	93.6	105.3	104.7	104.3
$E_{Tot.}$	−12.11	−10.30	−7.09	−7.38	−6.96	−7.25	−5.74	−6.28

[a] Oxygen in the same plane as the neighboring molecule. [b] Potential **1** multipole expansion up to hexadecapole. Potential **2** multipole expansion up to dipole. [c] Intermolecular coordinates optimization. [d] Full optimization.

TABLE 10: Distances (Å), Angles (deg), and Corrected Energies (kcal/mol) for a Formaldehyde Trimer (Conformations with 1 and 2 *Planar Bonds*[a])

	one *planar bond*[a]				two *planar bonds*[a]			
	potential **2**[b]	potential **1**[b]	631++G(2d,2p)[c]	631++G(2d,2p)[d]	potential **2**[b]	potential **1**[b]	631++G(2d,2p)[c]	631++G(2d,2p)[d]
$r_{C_1C_5}$	3.5472	3.4160	3.9918	3.9953	4.6023	4.1227	4.4648	4.4445
$\alpha_{C_5C_1O_2}$	92.7	99.6	98.4	98.2	92.2	94.0	87.7	87.6
$\alpha_{O_6C_5C_1}$	11.8	34.9	13.0	13.6	23.4	47.8	17.1	17.2
$r_{C_5C_9}$	3.4371	3.4182	3.1937	3.1783	3.4771	3.3888	3.1715	3.1504
$\alpha_{C_9C_5O_6}$	85.6	100.0	82.0	82.0	86.7	100.8	81.4	81.4
$\alpha_{O_{10}C_9C_5}$	24.1	34.2	54.8	54.8	21.7	36.2	55.5	55.4
$E_{Tot.}$	−10.17	−9.75	−6.98	−7.36	−8.53	−8.53	−6.91	−7.38

[a] Oxygen in the same plane as the neighboring molecule. [b] Potential **1** multipole expansion up to hexadecapole. Potential **2** multipole expansion to up dipole. [c] Intermolecular coordinates optimization. [d] Full optimization.

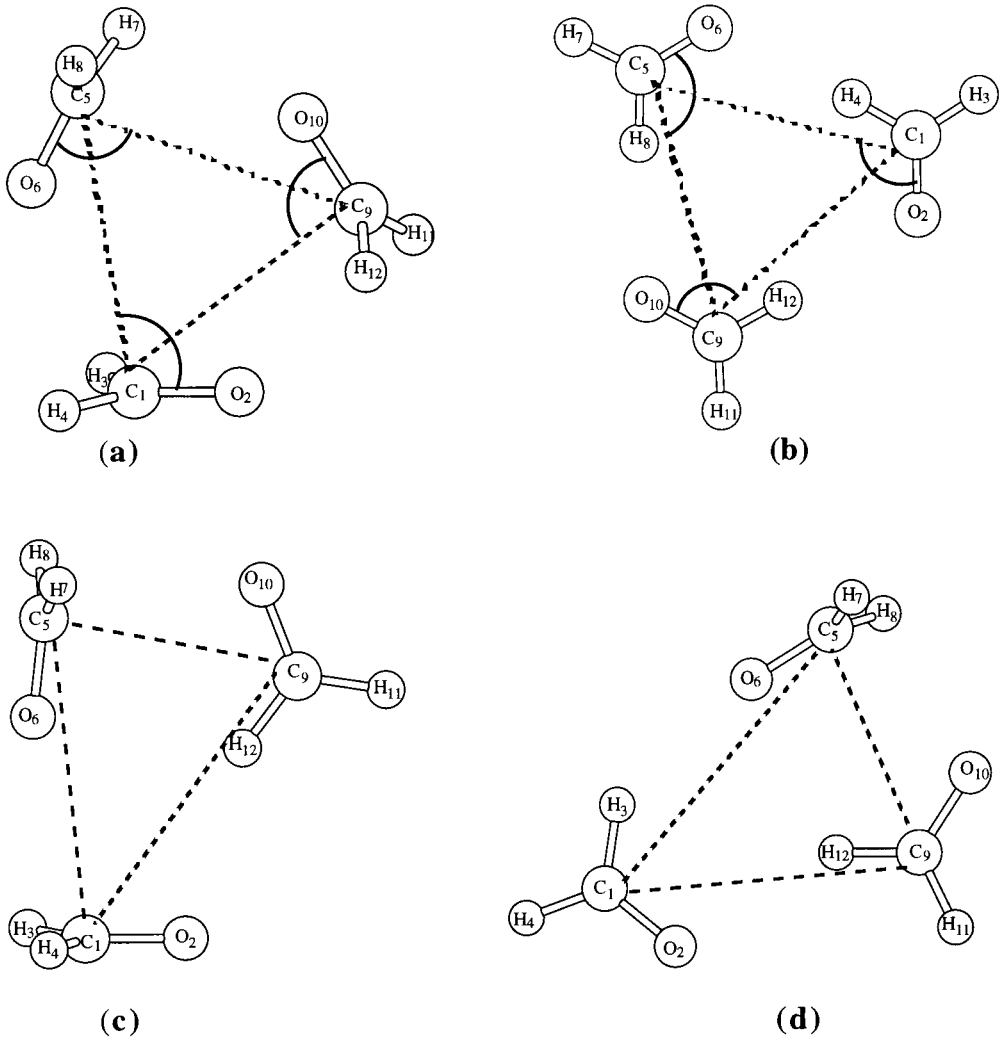

Figure 4. Stationary points for the formaldehyde trimer complex. (a) No *planar bonds*. (b) Three *planar bonds*. (c) One *planar bonds*. (d) Two *planar bonds* (*Planar bond*: structure where an oxygen atom is in the same plane as the neighboring molecule).

as the likely result of the above-mentioned significant effect on the energies of relaxing intramolecular coordinates in the more planar conformations. The original sequence might be restored if the BSSE is used in the ab initio optimization since, in the less planar conformations, molecules are closer to one another so they will be influenced to a greater extent by this error (in other words, they will be the farthest from the intermolecular minimum obtained in the absence of BSSE). The potentials lead to greater energy differences and absolute energy values than do the ab initio calculations. To assess the influence of the basis set on the energies, we carried out two specific calculations by using the aug-cc-pTVZ basis set and the fully optimized geometries of the stationary points for conformers in 4b and 4a, with three and zero *planar bonds*. The energies thus obtained were −6.82 kcal/mol for 4b and −8.28 kcal/mol for 4a, both of which are closer to those predicted from the potentials, which, however, are still more negative.

Simulation of the Liquid Phase

We conducted a molecular dynamics simulation under periodic boundary conditions[45] in a canonical ensemble, using the program MOLSIM.[55] The simulated system consisted of 512 formaldehyde molecules in a cubic box of 31.51 Å long edges. This is the box size needed to reproduce an experimental density of 0.815 g/cm^3 at 252.15 K—the temperature at which the simulation was performed. A center-of-mass interaction cutoff of 15.7 Å was applied. The equations of motion for the rigid molecules were integrated using quaternions together with a velocity Verlet algorithm. The time step was 2 fs, and the overall duration of the simulation 20 ps, with a prior equilibration for 6 ps. Induction interactions were calculated by using a self-consistent iterative process every 5 simulation steps. No reported data for formaldehyde in the liquid phase were found, so the compound was only compared in qualitative terms with other molecules bearing some common feature.

The mean potential energy was −5.30 kcal/mol, of which −2.95 kcal/mol corresponded to electrostatic and induction interactions, and the remainder, −2.35 kcal/mol, to dispersion and repulsion interactions. As can be seen, the dispersion energy was relatively similar to the electrostatic energy since the induction term ranged from −0.36 to −0.60 kcal/mol. Assuming ideal gas behavior for vapor formaldehyde, the heat of vaporization predicted by the potential is −5.80 kcal/mol, which agrees (2% lower) with the experimental[56] result (−5.92 kcal/mol).

Radial Distribution Functions. Figure 5 shows the atom−atom correlation functions for every possible atom pair in formaldehyde. As can be seen, the graphs are noiseless and well-defined. Some include a small shoulder in addition to the main peak. The O−O pair gives a shoulder at 3.45 Å, and the integration of the small, adjacent valley gives a coordination number of 1.8. This suggests that the first two neighbors are arranged in a different way relative to the molecule than are

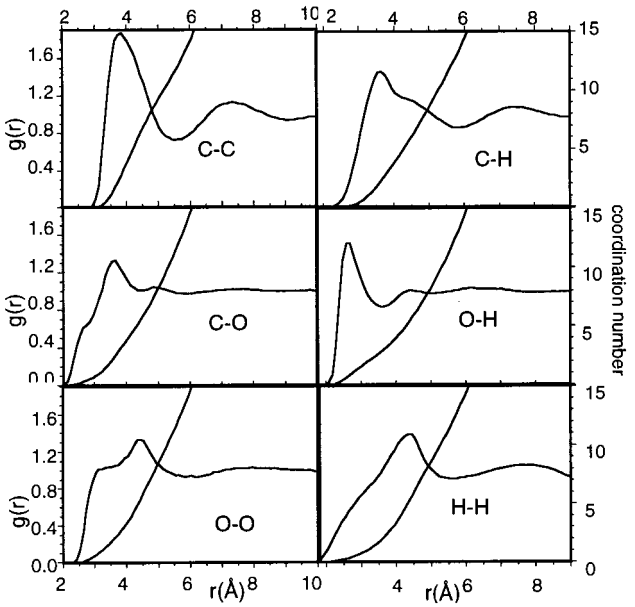

Figure 5. Atom−atom radial distribution functions and coordination numbers.

the other constituents of the first coordination sphere. This behavior is similar to that reported for acetone.[57] The graph for the O−H pair exhibits a peak at 2.70 Å integration of which as far as its minimum at 3.65 Å gives a coordination number of 2.77 that is equivalent to the number of hydrogen bonds.[28,49] This excludes the C_{2h} planar dimer and points at the C_s dimer, which possesses two distances of 2.70 and 2.82 Å and a third one of 4.29 Å.

Integration of the first minimum beyond the main peak—the second for $g_{O-H}(r)$ since the first describes hydrogen bonds—gives coordination numbers of 16, 15, 13.5, 12.5, 11.5, and 8 for the O−O, C−O, C−H, H−H, C−C and O−H pair, respectively. We may assume the center−center function to be accurately estimated by the $g_{C-C}(r)$ function. As can be seen, the values are generally close to those provided by the $g_{C-C}(r)$ function. These values are similar to those reported for formaldehyde−water[14] and for other molecules of the same type that involve hydrogen bonding to an oxygen atom in a carbonyl group.[57,58]

Cosine Distributions. To improve our understanding of the aggregates formed in the first-coordination sphere of a formaldehyde molecule in the liquid phase, we calculated the cosine distribution between a central molecule and its neighbors. Figure 6a shows the cosine distribution for the angle between the axes that join the hydrogens in a molecule and those in its neighbors. The distribution was calculated at different distances corresponding to also different coordination numbers. Figure 6b shows the distribution for the angle between the H···H axis and the vector joining the centers-of-mass of both molecules. Finally, Figure 6c shows a similar distribution where the H···H axis was replaced with that formed with the C−O bond, at a single distance (3.35 Å).

On the basis of the information provided by the three graphs, the possibility of a predominant dimer conformation can be excluded. All this suggests that the type of structure possibly involved is 1 order higher than the dimer and that the aggregates formed include both the C_s dimer and, possibly, C_{2h} structures. This is supported by the fact that new maxima at 180° and −180°, different from the maximum at a correlation order of 1, arise at correlation orders of 3 and 4, and also to a lesser extent at 2, in Figure 6b. Trimer structures of the types shown

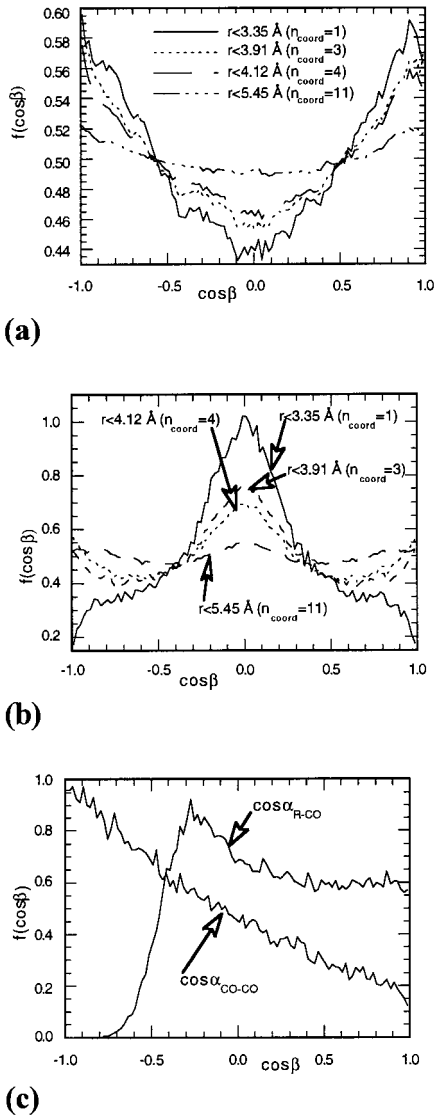

Figure 6. Cosine distributions of the angle between (a) H−H vectors, (b) H−H vector and the intermolecular vector, (c) C−O vectors, and the C−O vector and intermolecular vector (at 3.35 Å) of the central and neighboring formaldehyde molecules.

in Figure 4a might also occur. It should be noted that, on the basis of these figures, the first-coordination sphere is more structured than that in other systems such as acetone or acetonitrile.[8]

Dipole Moment. The dipole moment obtained in the gas phase was 2% greater than the experimental value. As can be seen from Figure 7a, the average induced dipole moment was 0.097 au; however, the peak was very broad and encompassed values from 0.035 to 0.17 au. From Figure 7b it seemingly follows that the angle between the permanent and induced dipole moments is about 18°, in most instances. It behaves similarly to that of acetone—this, however, exhibits a wider angle and also wider peak. By contrast, Jedlovszky and Pálinkás[57] showed that the most likely arrangement between the induced and permanent dipole moments is a parallel one. In view of these results, we shall assume the total dipole moment to be the sum of the induced moment and the gas-phase moment. This increases the dipole moment value by about 10%, which is small relative to other systems involving hydrogen bonding (e.g., acetone, acetonitrile, and water).[30] This may be the result of a smaller number of atoms in the molecule and also of a strong

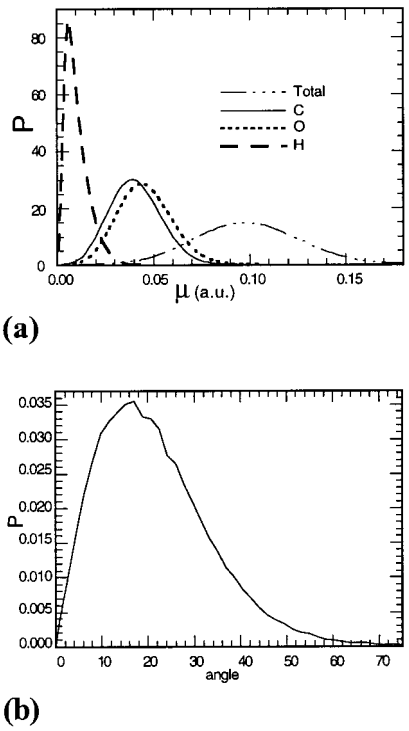

Figure 7. (a) Distribution of absolute values of the induced dipole moments (total and atom components). (b) Orientation of the induced moment relative to the fixed dipole.

accumulation and concentration of charge on the double bond of the carbonyl group.

Figure 7a shows the induced moment distributions for the different types of atoms. As expected, the hydrogens contribute little induction energy. It is the heavier atoms that produce the strongest induction effects—particularly the oxygen. It should be noted that the combination of all induced moments leads to a much wider distribution than do its individual components.

Conclusions

We constructed a potential where the interaction energy is a combination of several terms. The models used, which have specific physical significance, are consistent with the ab initio terms from which they are derived. The calculated total interaction energy follows the same trend as MP2 energies obtained from supermolecule calculations. The accuracy could be improved by including additional parameters to consider anisotropic effects on overlap and repulsion, as well as damping of induction effects or even intramolecular relaxation.

The minima and stationary points predicted from the potential are quite correct; the model predicts that the minimum with the most negative energy has a C_s conformation where the monomers lie perpendicular to each other, consistent with previous theoretical and experimental results. A second minimum of less negative energy and C_{2h} symmetry also appears. These results are consistent with the ab initio calculations performed in this work. Although the absolute energies obtained from the potentials are slightly more negative, the differences between the minima remain similar to the ab initio calculations.

The minimum obtained by Ford et al. using a smaller size basis set appears as a stationary point but not a minimum with the proposed models. The ab initio calculations show that, with the basis set used in this work, the conformation is a transition state.

From the contribution of each term to the minima it follows that the minimum with the largest negative energy is a combination of electrostatic and van der Waals interactions; however, contributions to the C_{2h} minimum are largely electrostatic.

One of the preliminary calculations on the trimer revealed that the structures predicted from the potential are consistent with the energies and structures provided by the ab initio calculations. From the latter and those for the dimer it follows that intramolecular coordinates are energetically more influential in the planar structures than those in the nonplanar ones.

Correlation and cosine distribution functions in the liquid phase reveal that the occurrence of a C_s dimer as an independent aggregate is unlikely as such a dimer would tend to be included in a larger aggregate. They also suggest the occurrence of various types of conformations in the aggregates. The number of molecules in the first-coordination sphere is about 13; also, the sphere appears to be more structured than that in other molecules such as acetone.

The liquid-phase dipole moment is about 10% greater than its gas-phase counterpart. The most likely angle between the permanent and induced dipole moments is approximately 18°, so nearly the whole induced dipole moment adds up to the permanent one. The highest contribution to induction is from the heavier atoms in the molecule.

Acknowledgment. We are pleased to acknowledge financial support of this research from (XUGA20903A98). J.M.H.-R. is also grateful to Xunta de Galicia for the award of a research grant. Time allocation for calculations was generously provided by the Centro de Supercomputación de Galicia (GESGA).

References and Notes

(1) Jorgensen, W. L. *J. Am. Chem. Phys.* **1979**, *101*, 2011.
(2) Karlström, G.; Linse, P.; Jönsson, B. *J. Am. Chem. Phys.* **1983**, *105*, 377.
(3) Niesar, U.; Corongiu, G.; Clementi, E.; Kneller, G. R.; Bhattacharya, D. K. *J. Phys. Chem.* **1990**, *94*, 7949.
(4) Millot, C.; Stone, A. J. *Mol. Phys.* **1992**, *77*, 439.
(5) Anwander, E. H. S.; Probst, M. M.; Rode, M. R. *Chem. Phys.* **1992**, *166*, 341.
(6) Astrand, P.-O.; Wallqvist, A.; Karlström, G. *J. Chem. Phys.* **1994**, *100*, 1262.
(7) Jedlovszky, P.; Turi, L. *J. Phys. Chem. A* **1997**, *101*, 2662.
(8) Cabaleiro-Lago, E. M.; Ríos, M. R. *J. Phys. Chem. A* **1997**, *101*, 1262.
(9) Dimitrova, Y.; Peyerimhoff, S. G. *J. Phys. Chem.* **1993**, *97*, 12731.
(10) Swaminathan, S.; Whitehead, R. J.; Guth, E.; Beveridge, D. L. *J. Am. Chem. Soc.* **1977**, *99*, 7817.
(11) Vos, R. J.; Hendriks, R.; Duijneveldt, F. B. *J. Comput. Chem.* **1990**, *11*, 1.
(12) Mühlbauer, W. C. F.; Damewood, J. R. J. *J. Phys. Chem.* **1988**, *92*, 3693.
(13) Ramelot, T. A.; Hu, C.; Fowler, J. E.; DeLeeuw, B. J.; Schaefer-III, H. F. *J. Chem. Phys.* **1994**, *100*, 4347.
(14) Mehrotra, P. K.; Beveridge, D. L. *J. Am. Chem. Soc.* **1980**, *102*, 4287.
(15) Blair, J. T.; Krogh-Jerpersen, K.; Levy, R. M. *J. Am. Chem. Soc.* **1989**, *111*, 6948.
(16) Lovas, F. J.; Suenram, R. D.; Coudert, L. H.; Blake, T. A.; Grant, K. J.; Novick, S. E. *J. Chem. Phys.* **1990**, *92*, 891.
(17) Nelander, B. *J. Chem. Phys.* **1980**, *73*, 1034.
(18) Khoskhoo, H.; Nixon, E. R. *Spectrochim. Acta* **1973**, *29A*, 603.
(19) Del-Bene, J. E. *J. Chem. Phys.* **1974**, *60*, 3812.
(20) Frurip, D. J.; Curtiss, L. A.; Blander, M. *J. Phys. Chem.* **1978**, *82*, 2555.
(21) Kemper, M. J.; Hoeks, C. H.; Buck, H. M. *J. Chem. Phys.* **1981**, *74*, 5744.
(22) Hobza, P.; Mehlorn, A.; Carsky, P.; Zahradnik, R. *J. Mol. Struct. (THEOCHEM)* **1986**, *138*, 387.
(23) Ford, T. A.; Glasser, L. *J. Mol. Struct. (THEOCHEM)* **1997**, *398*−*399*, 381.
(24) Weng, S.-X.; Torrie, B. H.; Powell, B. M. *Mol. Phys.* **1989**, *68*, 25.
(25) Hobza, P.; Zahradník, R. *Intermolecular Complexes*; Elsevier:, New York, 1988.

(26) Jeziorski, B.; Moszynski, R.; Szalewicz, K. *Chem. Rev.* **1994**, *94*, 1887.
(27) Hayes, I. C.; Stone, A. J. *Mol. Phys.* **1984**, *53*, 83.
(28) Chalasinski, G.; Szczesniak, M. M. *Chem. Rev.* **1994**, *94*, 1723.
(29) Stone, A. J.; Price, S. L. *J. Phys. Chem.* **1988**, *92*, 3325.
(30) Wallqvist, A.; Ahlström, P.; Karlström, G. *J. Phys. Chem.* **1990**, *94*, 1649.
(31) van-Duijnefeldt, F. B.; van-Duijnefeldt-van-de-Rijdt, J. G. C. M.; van-Lenthe, J. H. *Chem. Rev.* **1994**, *94*, 1873.
(32) Gutowski, M.; Szczesniak, M. M.; Chalasinski, G. *Chem. Phys. Lett.* **1995**, *241*, 140.
(33) Boys, S. F.; Bernardi, F. *Mol. Phys.* **1970**, *19*, 553.
(34) Hayes, I. C.; Stone, A. J. *Mol. Phys.* **1984**, *53*, 107.
(35) Stone, A. J.; Tough, R. J. A. *Chem. Phys. Lett.* **1984**, *110*, 123.
(36) Del-Bene, J. E. *J. Chem. Phys.* **1987**, *86*, 2110.
(37) Hermida-Ramön, J. M.; Ríos, M. A. *J. Phys. Chem. A* **1998**, *102*, 2594.
(38) Grey, C.; Gubbins, K. E. *Theory of Intermolecular Fluids*; Clarendon: Oxford, 1984; Vol. 1.
(39) Sadlej, A. J. *J. Mol. Struct. (THEOCHEM)* **1991**, *80*, 234.
(40) Amos, R. D.; Alberts, I. L.; Andrews, J. S.; Colwell, S. M.; Handy, N. C.; Jayatilaka, D.; Knowles, P. J.; Kobayashi, R.; Laiding, K. E.; Laming, G.; Lee, A. M.; Maslen, P. E.; Murray, C. W.; Rice, J. E.; Simandiras, E. D.; Stone, A. J.; Su, M.-D.; Tozer, D. J. CADPAC: The Cambridge Analytic Derivates Package Issue 6, Cambridge, 1995.
(41) Stone, A. J. *Chem. Phys. Lett.* **1981**, *83*, 233.
(42) Stone, A. J.; Alderton, M. *Mol. Phys.* **1985**, *78*, 1047.
(43) Seur, C. R. L.; Stone, A. J. *Mol. Phys.* **1993**, *78*, 1267.
(44) Frisch, M. J.; Trucks, G. W.; Schlegel, H. B.; Gill, P. M. W.; Johnson, N. G.; Robb, M. A.; Cheeseman, J. R.; Keith, T.; Petersson, G. A.; Montgomery, J. A.; Raghavachari, K.; Al-Laham, M. A.; Zakrzewski, V. G.; Ortiz, J. V.; Foresman, J. B.; Cioslowski, J.; Stefanov, B. B.; Nanayakkara, A.; Challacombe, M.; Peng, C. Y.; Ayala, P. Y.; Chen, W.; Wong, M. W.; Andres, V.; Replogle, E. S.; Gomperts, R.; Martin, R. L.; Fox, D. J.; Binkley, J. S.; Defrees, D. J.; Baker, J.; Stewart, V.; Head-Gordon, M.; Gonzalez, C.; Pople, J. A. Gaussian 94, Revision C.3; Gaussian, Inc., Pittsburgh, PA, 1995.
(45) Allen, M. P.; Tildesley, D. J. *Computer Simulation of Liquids*; Clarendon Press: Oxford, 1987.
(46) Stone, A. J. *The Theory of Intermolecular Forces*; Clarendon Press: Oxford, 1996.
(47) Price, S. L.; Stone, A. J.; Alderton, M. *Mol. Phys.* **1984**, *52*, 987.
(48) Stone, A. J.; Tong, C.-S. *J. Comput. Chem.* **1994**, *15*, 1377.
(49) Tang, T. K.; Toennis, J. P. *J. Chem. Phys.* **1984**, *80*, 3726.
(50) Stone, A. J.; Dullweber, A.; Popelier, P. A. L.; Wales, D. J. Orient: a program for studing interactions between molecules. Version 3.2. University of Cambridge, 1995.
(51) Engdahl, A.; Nelander, B.; Astrand, P.-O. *J. Chem. Phys.* **1993**, *99*, 4894.
(52) Bercovici, T.; King, J.; Becker, K. S. *J. Chem. Phys.* **1971**, *56*, 3959.
(53) Desiraju, G. R. *Acc. Chem. Res.* **1996**, *29*, 441.
(54) Allen, F. H.; Lommerse, J. P. M.; Hoy, V. J.; Howard, J. A. K.; Desiraju, G. R. *Acta Crystallogr.* **1996**, *B52*, 734.
(55) Linse, P.; Wallqvist, A. MOLSIM 1.2 Lund University, Sweden, 1991.
(56) Weast, R. C.; Astle, M. J.; Beyer, W. H. *CRC Handbook of Chemistry and Physics*, 64th ed.; CRC Press: Boca Raton, FL, 1983−1984.
(57) Jedlovszky, P.; Pálinkás, G. *Mol. Phys.* **1995**, *84*, 217.
(58) Jedlovszky, P.; Turi, L. *J. Phys. Chem. B* **1997**, *101*, 5429.